JCTC Journal of Chemical Theory and Computation

Singlet−Triplet Transitions in Real-Time Time-Dependent Hartree−Fock/Density Functional Theory

Christine M. Isborn and Xiaosong Li*

Department of Chemistry, University of Washington, Seattle, Washington 98195-1700

Received May 23, 2009

Abstract: Real-time time-dependent Hartree−Fock (TDHF)/density functional theory (TDDFT) has been gaining in popularity because of its ability to treat phenomena beyond the linear response and because it has the potential to be more computationally powerful than frequency domain TDHF/TDDFT. Within real-time TDHF/TDDFT, we present a method that gives the excited state triplet energies starting from a singlet ground state. Using a spin-dependent field, we break the spin-symmetry of the α and β density matrices, which incorporates a triplet contribution into the superposition state. The α electron density follows the applied field, and the β electron density responds to the perturbation from the changing α electron density. We examine the individual α/β responses during the electron density propagation. Singlet−triplet transitions appear as 'dark' states: they are present in the α/β responses but are absent from the total electron density response.

Introduction

Investigation of electronic excitations is of fundamental importance in spectroscopy and photochemistry. Not only is accurate understanding of the photoallowed transitions necessary, but because much photochemistry also occurs on electronic surfaces that are not directly photoaccessible, such as triplet states, it is also of great importance to accurately model these 'dark' states. Because of their affordability and generally good accuracy, single configuration excited state methods such as time-dependent Hartree−Fock (TDHF)[1−4] and density functional theory (TDDFT)[5,6] have become the modern-day workhorses for modeling electronic excitations. While the majority of TDHF and TDDFT calculations are performed within the linear response matrix formalism in the frequency domain,[1,2,7,8] real-time methods are gaining in popularity because of their ability to treat phenomena beyond the linear response and because they have the potential to be more computationally efficient for large-scale systems when a large matrix equation must be solved in the frequency domain.[9−18]

While the matrix formalism of linear response TDHF/TDDFT can easily include transitions from a reference ground state singlet to triplets, singlet−triplet transitions are generally not accessible within real-time TDHF/TDDFT approaches because the applied perturbation is often spin-independent, and the α and β electron density responses are identical. With a spin-independent perturbation, such as the ubiquitous electric field within the dipole approximation, both the α and β electron densities are simultaneously excited, maintaining a closed-shell singlet state. The resulting perturbed wave function is then a superposition of the singlet reference ground state with other excited singlet states.[19] However, no contribution from any triplet state is included in the superposition.

In the present investigation, we show that a spin-dependent perturbation within real-time TDHF/TDDFT incorporates triplets into the superposition state wave function. This can be done via a spin-dependent field,[14] in which only the α electron density directly experiences the applied perturbation. Because the α and β electron densities are coupled through the Coulomb and exchange (for HF)/exchange-correlation (for DFT) terms, the β electron density is then perturbed by the change in the α electron density, leading to breaking of the singlet spin-symmetry and incorporation of the triplet wave function. We monitor the coupled α and β electron density response and the time-dependent expectation value of S^2.

Method

In our real-time electron dynamics, we use the method described in refs 12, and 19−22 in which the electron density

* Corresponding author e-mail: li@chem.washington.edu.

10.1021/ct900264b CCC: $40.75
Published on Web 08/12/2009

is propagated in the time domain and the time-dependent Hamiltonian takes into account the evolving electron distribution. We use atomic units consistently throughout this paper, where $m_e = \hbar = 1$. The TDHF/TDDFT equation for the density matrix is given by

$$i\frac{d\mathbf{P}(t)}{dt} = [\mathbf{F}(t), \mathbf{P}(t)] \tag{1}$$

where $\mathbf{P}$ and $\mathbf{F}$ are density and Fock/Kohn−Sham (KS) matrices. The MOs are represented as a linear combination of atomic orbital basis functions χ_μ as $\varphi_i(t) = \Sigma_\mu c_{\mu,i}(t)\chi_\mu$. The density matrix $\mathbf{P}(t)$ has elements given by the product of the time-dependent coefficients $P_{\mu\nu}(t) = \Sigma_i c^\dagger_{\mu,i}(t)c_{\nu,i}(t)$. In the unrestricted TDHF/TDDFT electron dynamics, the α and β electron densities are propagated with coupled α and β Fock/KS operators. With a spin-dependent perturbation, the α and β Fock matrices are

$$\mathbf{F}^\alpha(t) = \mathbf{h} + \mathbf{J}[\boldsymbol{\rho}^\alpha(t) + \boldsymbol{\rho}^\beta(t)] - \mathbf{K}[\boldsymbol{\rho}^\alpha(t)] + V_{ext} \tag{2}$$

$$\mathbf{F}^\beta(t) = \mathbf{h} + \mathbf{J}[\boldsymbol{\rho}^\alpha(t) + \boldsymbol{\rho}^\beta(t)] - \mathbf{K}[\boldsymbol{\rho}^\beta(t)] \tag{3}$$

where $\mathbf{h}$, $\mathbf{J}$, and $\mathbf{K}$ are the core Hamiltonian, two-electron Coulomb, and exchange matrices. For the KS matrices, $\mathbf{K}$ is replaced by the exchange-correlation potential $\mathbf{V}_{xc}$. V_{ext} is an external perturbation applied to α electrons only. In this work we include a spin-dependent perturbation within the Hamiltonian by adding the field term $\mathbf{E}(t) = \mathbf{E}_{max}\mathbf{d}\sin(\omega t)$ to the α Fock/KS matrix $\mathbf{F}^\alpha(t)$, where $\mathbf{d}$ is the electric dipole integral $d_{\mu\nu} = \langle\chi_\mu|\hat{r}|\chi_\nu\rangle$.

The electron density is propagated with a midpoint unitary transformation written in terms of the eigenvectors $\mathbf{C}$ and eigenvalues ε of the time-dependent Fock/KS matrix at time t_k

$$\mathbf{P}(t_{k+1}) = \mathbf{U}(t_k)\mathbf{P}(t_{k-1})\mathbf{U}^\dagger(t_k) \tag{4}$$

$$\begin{aligned}\mathbf{U}(t_k) &= \exp(i\mathbf{F}(t_k)2\Delta t)\\ &= \mathbf{C}(t_k)\exp(i\varepsilon(t_k)2\Delta t)\mathbf{C}^\dagger(t_k)\end{aligned} \tag{5}$$

This unitary transformation propagation naturally retains the idempotency of the density matrix ($\mathbf{P}\cdot\mathbf{P} = \mathbf{P}$).

In real-time TDHF/TDDFT electron dynamics, a perturbation to the ground state orbitals, φ, mixes occupied and virtual molecular orbitals (MOs) to give rise to a set of perturbed orbitals, φ', and a superposition state, ψ'

$$\phi' = \sum_i a_i\phi_i \tag{6}$$

$$\psi' = |\phi'_1\phi'_2....\phi'_N| \tag{7}$$

We have previously shown that this superposition state includes not only singly excited states but also doubly excited states within a closed-shell configuration, when using a spin-independent perturbation.[19] With a spin-dependent perturbation (eqs 2 and 3), the α and β spatial components of the wave function are no longer identical. We herein use a two-electron, two-orbital system with bonding MO φ_σ and virtual MO φ_{σ^*}, beginning in S_0, with both electrons in φ_σ, to show how the triplet component is introduced into the superposition wave function. The single-configuration superposition state ψ' in eq 7 can be written as (where $\mathbf{r}$ and τ are spatial and spin variables, respectively)

$$\begin{aligned}\psi' &= \frac{1}{\sqrt{(1+c_\alpha^2)(1+c_\beta^2)}}|\phi'(\mathbf{r}_1)\alpha(\tau_1)\phi'(\mathbf{r}_2)\beta(\tau_2)|\\ &= \frac{1}{\sqrt{(1+c_\alpha^2)(1+c_\beta^2)}}\times\\ &\quad |[\phi_\sigma + c_\alpha\phi_{\sigma^*}](\mathbf{r}_1)\alpha(\tau_1)[\phi_\sigma + c_\beta\phi_{\sigma^*}](\mathbf{r}_2)\beta(\tau_2)|\\ &= \frac{1}{\sqrt{(1+c_\alpha^2)(1+c_\beta^2)}}\left(\psi_{S_0} + \left(\frac{c_\alpha + c_\beta}{\sqrt{2}}\right)\psi_{S_1} + \left(\frac{c_\beta - c_\alpha}{\sqrt{2}}\right)\psi_{T_0} + c_\alpha c_\beta\psi_{S_2}\right)\end{aligned} \tag{8}$$

Here ψ_{S_1} and ψ_{T_0} are the spin-adapted singlet and triplet configurations, and ψ_{S_2} is the doubly excited configuration. The coefficients c_α and c_β determine the degree of individual α and β perturbation from the ground state and are governed by both the strength of the spin-dependent perturbation and the system-dependent response. Eq 8 indicates that a spin-dependent perturbation gives rise to a mixing of triplet component in the superposition state.[23]

Because the field is applied only to the α electron density, the spin-symmetry is broken from a pure singlet state, and we have an unrestricted wave function, whose spin-symmetry time evolution can be monitored by the time-dependent expectation value of the squared total spin angular momentum operator $\hat{S}^2$. For a single determinant open-shell wave function in an orthonormal basis, $\langle\hat{S}^2(t)\rangle$ can be written in terms of the time-dependent density matrices as[24,25]

$$\langle\hat{S}^2(t)\rangle = \left(\frac{N_\alpha - N_\beta}{2}\right)^2 + \frac{N_\alpha + N_\beta}{2} - \mathrm{Tr}[\mathbf{P}_\alpha(t)\cdot\mathbf{P}_\beta(t)] \tag{9}$$

Because $\hat{S}^2 = 0$ for singlets, such as S_0, S_1, and S_2, and $\hat{S}^2 = 2$ for triplets, such as T_0, a nonzero $\hat{S}^2$ value in eq 9 becomes an indicator of the singlet−triplet mixing during the time-evolution of the superposition wave function.

Results and Discussion

The development version of the Gaussian code[26] is used to obtain the initial wave function and to calculate the one- and two-electron integrals. We use a minimal STO-3G basis set for simplicity of analysis and also a 6-31G(d,p) basis for comparison. The simulations begin with the molecule initially in its field-free ground state. The electric field vector is applied along the molecular (z) axis for three cycles with a frequency of $\omega = 0.06$ au. We use an integration time step of 0.002 fs and propagate the electron density for 50 fs. As we and other groups have shown,[19,27] shifting of transition energies can also occur when contributions from excited states in the superposition state become large. For the spin-dependent perturbations discussed herein, a stronger field or a field frequency closer to resonance not only shifts the peak energies but also can cause extreme broken spin symmetry, with $\langle\hat{S}^2(t)\rangle$ values approaching 1. The intensity of peaks in

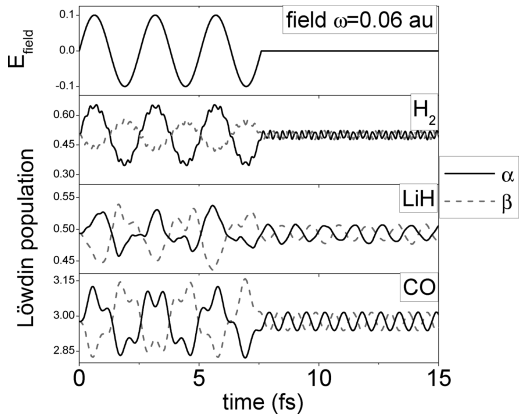

Figure 1. Electric field and Löwdin populations. Top panel: applied electric field with $\omega = 0.06$ au. Other panels: α and β Löwdin populations on one atom of the diatomics H_2, LiH, and CO. The α population (black lines) follows the field, and the β population (gray dash lines) responds by shifting onto the other atom. This breaks the spin-symmetry of the system, creating a superposition state that includes triplet contributions. After the field is off, the α and β populations oscillate at the same frequencies but out of phase with each other.

the spectrum is directly related to population of various states in the superposition wave function, making the strength of the spin-dependent perturbation directly correlated to these intensities. In order to compare peak energies with those obtained from linear response theory, we have kept the perturbation weak and away from resonant energies in order to not significantly alter the population away from that of the reference ground state.

A spin-dependent perturbation in the form of an off-resonant field was applied to the ground state of three different diatomic molecules: H_2, LiH, and CO. Figure 1 shows the applied electric field for $\omega = 0.06$ au, and the resulting Löwdin populations on one atom, obtained using the TDHF Hamiltonian with the STO-3G basis. A field strength of $E_{max} = 0.1$ au was used for H_2, and $E_{max} = 0.01$ au was used for LiH and CO. Initially, the diatomics are closed-shell with identical α and β populations on each atom. Once the spin-dependent perturbation is applied, the α electron density (black lines) follows the field, building up electron density on one atom in each of the diatomics. The β electron density (gray dash lines) responds to the changing α electron density by decreasing on that atom, and building up on the other atom, breaking the spin-symmetry. Once the field is removed the magnitude of the α and β population oscillations decrease significantly, as the field is no longer directly driving the α electron density, and the β electron density no longer is responding to the large change in the α electron density. While the change in magnitude of the α and β populations is much smaller after the field is off, they continue to oscillate out of phase. It is this out-of-phase oscillation that indicates the triplet contribution within the superposition state, as suggested by eq 8.

As discussed in the previous section, the $\langle \hat{S}^2 \rangle$ value is an indicator of the singlet−triplet mixing in the superposition state. The corresponding $\langle \hat{S}^2 \rangle$ values during the dynamics are shown in Figure 2. A nonzero value clearly indicates that the superposition state is no longer made up of pure singlets,

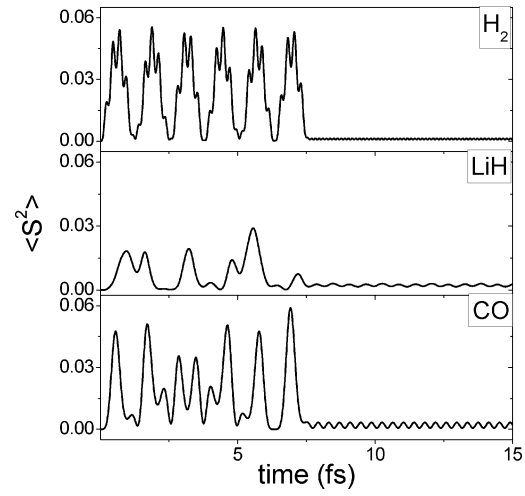

Figure 2. $\langle \hat{S}^2 \rangle$ value for H_2, LiH, and CO, using the same field conditions as given in Figure 1. The magnitude of $\langle \hat{S}^2 \rangle$ represents the triplet contribution to the superposition state.

and the magnitude of $\langle \hat{S}^2 \rangle$ indicates the degree of triplet contribution to the superposition state wave function. Because $\langle \hat{S}^2 \rangle$ is calculated as the trace of the product of the α and β electron densities, see eq 9, the value takes into account the phase of the wave function from the imaginary part of the density matrix. With the same field conditions as for the populations given in Figure 1, the value of $\langle \hat{S}^2 \rangle$ remains small throughout the dynamics. For H_2, using a maximum field strength of $E_{max} = 0.1$ au, the maximum value of $\langle \hat{S}^2 \rangle$ during the field application was 0.056 and was 0.0014 once the field was removed. For LiH and CO, with $E_{max} = 0.01$ au, the maximum of $\langle \hat{S}^2 \rangle$ with the field on was 0.029 and 0.059, respectively, and after field removal it was 0.0032 and 0.0033. A weaker field was used because the LiH and CO transition energies are closer to the $\omega = 0.06$ au field frequency, leading to a larger response.

Despite the α and β Löwdin populations oscillating out-of-phase with each other, eq 8 indicating a triplet contribution to the wave function, and $\langle \hat{S}^2 \rangle$ no longer being zero, the Fourier transformation (FT) of the total residual dipole moment $\mathrm{Tr}[\mathbf{d} \cdot (\mathbf{P}^{\alpha}(t) + \mathbf{P}^{\beta}(t))]$ gives an absorption spectrum that agrees with the closed-shell singlet results, see Figure 3 (black lines). In the absorption spectrum of H_2 there is a single peak, which is at the $S_0 \rightarrow S_1$ transition energy of 0.94 au (Table 1). However, examinations of the individual α and β contributions to the total dipole moment show that the out-of-phase oscillation provides additional information. In addition to the FT of the total dipole moment, Figure 3 also shows the FT of the contribution of the α electron density to the total residual dipole moment (gray dash lines), calculated via $\mathrm{Tr}[\mathbf{d} \cdot \mathbf{P}^{\alpha}(t)]$. The FT of the β contribution is identical. For H_2, this 'absorption spectrum' shows a peak at the same $S_0 \rightarrow S_1$ transition energy but also an additional peak at 0.57 au, which corresponds to the linear response TDHF excitation energy from the S_0 state into the triplet T_0 state. This result shows that broken-spin real-time TDHF/TDDFT simulations yield the 'dark' transitions between singlet and triplet states in the individual α or β contributions to the total dipole moment. These 'dark' transitions do not show up in the total dipole allowed absorption spectrum, as

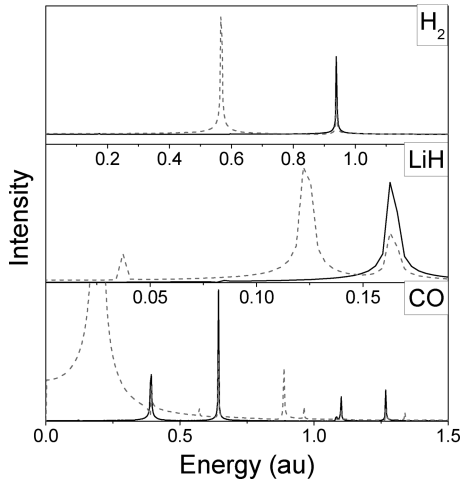

Figure 3. TDHF/STO-3G absorption spectra for H_2, LiH, and CO. Fourier transformation of the total dipole moment (black) shows dipole allowed singlet-to-singlet transitions. These peak energies agree with the closed-shell linear-response results (see Table 1). Fourier transformation of the α or β contribution to the dipole moment (gray dash) shows additional peaks corresponding to triplet transitions.

Table 1. Linear Response Excitation Energies (au)

	z-allowed singlet	triplet
	TDHF/STO-3G	
H_2	0.94	0.57
LiH	0.17	0.13
CO	0.64	0.20
	1.10	0.89
	1.27	1.13
	TDHF/6-31G(d,p)	
H_2	0.55	0.37
LiH	0.15	0.11
CO	0.54	0.22
	0.67	0.58
	0.95	0.77
	1.06	0.97
	TDPBE/STO-3G	
H_2	0.95	0.62
LiH	0.13	0.11
CO	0.64	0.31
	0.98	0.79
	1.14	1.00

the out of phase α/β oscillations cancel out in the total dipole response. This spin-dependent perturbation will only yield transitions in which the transition dipole matrix element $\langle\chi_\mu|\hat{r}|\chi_\nu\rangle$ is nonzero. While singlet−triplet transitions are not formally spin-symmetry allowed, the individual spin-allowed transitions for either the α or β electron can yield the singlet−triplet transitions as observed in the FT of the time evolution of the α or β electron density dipole moment. Just as with singlet−singlet transitions, the strength of the singlet−triplet transitions is governed by the magnitude of the dipole matrix element, and additional singlet−triplet transitions can be achieved by changing the field direction or using field terms beyond the dipole approximation.

The spectra for LiH and CO in Figure 3 are consistent with those found for the two-electron system H_2. For LiH, the FT of the α electron density dipole moment shows both the $S_0 \rightarrow S_1$ peak, and the $S_0 \rightarrow T_0$ peak, both of which are

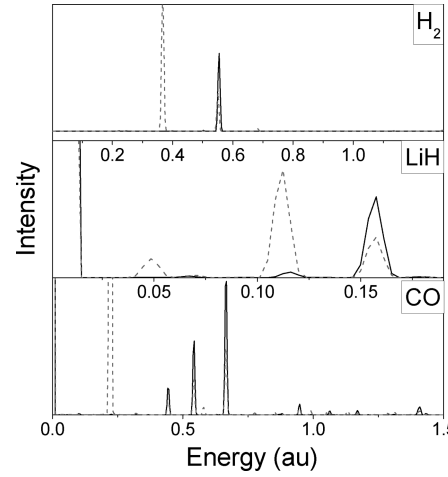

Figure 4. TDHF/6-31G(d,p) absorption spectra for H_2, LiH, and CO. Fourier transformation of the total dipole moment (black) shows dipole allowed singlet-to-singlet transitions. Fourier transformation of the α or β contribution to the dipole moment (gray dash) shows additional peaks corresponding to triplet transitions.

dominant HOMO−LUMO transitions. Because of a small population transfer into the excited state, the peak energies are slightly shifted from the linear response results (see Table 1). The dynamics give the $S_0 \rightarrow S_1$ transition energy at 0.16 au, and the $S_0 \rightarrow T_0$ transition energy at 0.12 au. There is also an additional small peak at 0.04 au which corresponds to transitions between the two excited states. This low-energy peak disappears at weaker field strengths. For CO the overall pattern is the same, with the FT of the α electron dipole moment showing both the singlet−singlet and the singlet−triplet transitions. The low energy transitions are $\pi \rightarrow \pi^*$, while the two higher energy transitions are $\sigma \rightarrow \sigma^*$. There is no shifting of peak transition energies compared to linear response theory, indicating very little population transfer. Because the $S_0 \rightarrow T_0$ transition at 0.20 au is near the field frequency of $\omega = 0.06$ au, the $S_0 \rightarrow T_0$ peak is very intense due to a larger T_0 contribution in the superposition state.

We also present two comparisons, one using the larger 6-31G(d,p) basis with the HF Hamiltonian (Figure 4) and the other using the same simple STO-3G basis with the PBE density functional Hamiltonian (Figure 5). The larger basis results show peaks shifting to lower energies as expected from linear response theory (Table 1). For the larger basis, we decreased the maximum field strength for H_2 and LiH to 0.03 au and 0.005 au, respectively. Because of the relatively large field strength of 0.01 au for CO, there is more population of the lower energy states, increasing the intensity of the corresponding lower energy peaks. The TDDFT results are comparable to those obtained with TDHF, with results agreeing with those from linear response theory (Table 1). The real-time TDDFT simulations used field conditions identical to the TDHF/STO-3G simulations. Some of the TDPBE excitations energies are different from the TDHF energies, changing the peak locations. Also, in addition to changes in the excitation energies, there are changes in the energies of peaks that correspond to transitions between excited states. For example, because the TDPBE LiH $S_0 \rightarrow T_0$ and $S_0 \rightarrow S_1$ transitions are closer in energy than the TDHF

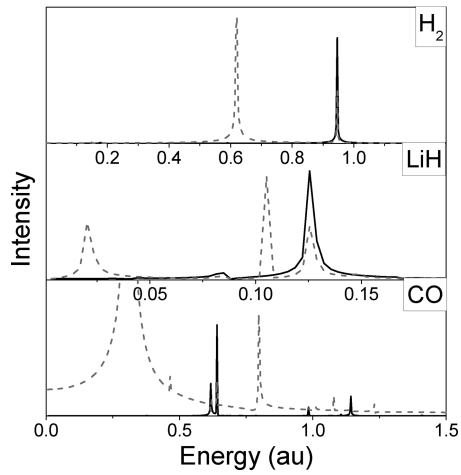

Figure 5. TDPBE/STO-3G absorption spectra for H_2, LiH, and CO. Fourier transformation of the total dipole moment (black) shows dipole allowed singlet-to-singlet transitions. Fourier transformation of the α or β contribution to the dipole moment (gray dash) shows additional peaks corresponding to triplet transitions.

transition energies, the peak due to transition between the excited states is red-shifted by ∼0.02 au compared to TDHF.

Conclusion

In this work we present a method that models singlet−triplet transitions within real-time TDHF and TDDFT methods. With the introduction of a spin-dependent perturbation, we show the incorporation of the triplet wave function into the superposition state achieved through real-time electron density propagation via monitoring of the α and β populations as well as the value of $\langle \hat{S}^2 \rangle$. With this mixed-spin superposition state, we observe both $S_0 \rightarrow$ singlet transitions and $S_0 \rightarrow$ triplet transitions as well as transitions between excited states.

Acknowledgment. Support is provided by NSF grants PHY-CDI 0835546 and CHE-CAREER 0844999 and the ACS Petroleum Research Fund (46487-G6). Enlightening discussions with Ernest Davidson are gratefully acknowledged.

References

(1) Simons, J. *J. Chem. Phys.* **1971**, *55*, 1218–1230.

(2) Jørgensen, P.; Simons, J. *Second quantization-based methods in quantum chemistry*; Academic Press: New York, 1981.

(3) Kulander, K. C.; Devi, K. R. S.; Koonin, S. E. *Phys. Rev. A* **1982**, *25*, 2968.

(4) Dreuw, A.; Head-Gordon, M. *Chem. Rev.* **2005**, *105*, 4009.

(5) Runge, E.; Gross, E. K. U. *Phys. Rev. Lett.* **1984**, *52*, 997.

(6) Petersilka, M.; Gossmann, U. J.; Gross, E. K. U. *Phys. Rev. Lett.* **1996**, *76*, 1212.

(7) Casida, M. E. *Recent Advances in Density-Functional Methods*; World Scientific: Singapore, 1995; pp 155−193.

(8) Stratmann, R. E.; Scuseria, G. E.; Frisch, M. J. *J. Chem. Phys.* **1998**, *109*, 8218.

(9) Yabana, K.; Bertsch, G. F. *Phys. Rev. B* **1996**, *54*, 4484.

(10) Tsolakidis, A.; Sánchez-Portal, D.; Martin, R. M. *Phys. Rev. B* **2002**, *66*, 235416.

(11) Marques, M. A. L.; López, X.; Varsano, D.; Castro, A.; Rubio, A. *Phys. Rev. Lett.* **2003**, *90*, 258101.

(12) Li, X.; Smith, S. M.; Markevitch, A. N.; Romanov, D. A.; Levis, R. J.; Schlegel, H. B. *Phys. Chem. Chem. Phys.* **2005**, *7*, 233.

(13) Smith, S.; Markevitch, A.; Romanov, D.; Li, X.; Levis, R.; Schlegel, H. *J. Phys. Chem. A* **2004**, *108*, 11063.

(14) Wang, F.; Yam, C. Y.; Chen, G.; Fan, K. *J. Chem. Phys.* **2007**, *126*, 134104.

(15) Wang, F.; Yam, C. Y.; Chen, G. *J. Chem. Phys.* **2007**, *126*, 244102.

(16) Andrade, X.; Botti, S.; Marques, M. A. L.; Rubio, A. *J. Chem. Phys.* **2007**, *126*, 184106.

(17) Takimoto, Y.; Vila, F. D.; Rehr, J. J. *J. Chem. Phys.* **2007**, *127*, 154114.

(18) Eshuis, H.; Balint-Kurti, G. G.; Manby, F. R. *J. Chem. Phys.* **2008**, *128*, 114113.

(19) Isborn, C. M.; Li, X. *J. Chem. Phys.* **2008**, *129*, 204107.

(20) Schlegel, H. B.; Smith, S. M.; Li, X. *J. Chem. Phys.* **2007**, *126*, 244110.

(21) Isborn, C. M.; Li, X.; Tully, J. C. *J. Chem. Phys.* **2007**, *126*, 134307.

(22) Li, X.; Tully, J. C. *Chem. Phys. Lett.* **2007**, *439*, 199.

(23) Schlegel, H. B. *Encyclopedia of Computational Chemistry*; Wiley: Chichester, 1998; pp 2665−71.

(24) Chen, W.; Schlegel, H. B. *J. Chem. Phys.* **1994**, *101*, 5957.

(25) Staroverov, V. N.; Davidson, E. R. *Chem. Phys. Lett.* **2000**, *330*, 161.

(26) Frisch, M. J. *Gaussian Development Version, Revision D.02*; Gaussian, Inc.: Wallingford, CT, 2004.

(27) Hu, C.; Sugino, O.; Miyamoto, Y. *Phys. Rev. A* **2006**, *74*, 032508.

CT900264B